Airgap Prediction: Use of Second-Order Diffraction and Multi-Column Models

Bert Sweetman and Steven R. Winterstein
Civil & Environmental Engineering Department, Stanford University, USA

Trond Stokka Meling
Statoil, Stavanger, Norway

Jørn Birknes
Det Norske Veritas, Høvik, Norway

ABSTRACT

The airgap of a specific semi-submersible platform subjected to irregular waves is considered. The effects of including second-order diffraction contributions are demonstrated, and the sensitivity of this analysis to numerical model complexity is investigated. Detailed model test results for both motions and airgap time histories are used to verify the analysis results. A new approach is proposed for use in post-processing second-order hydrodynamic transfer functions. In the new approach, those transfer functions that are unavailable or believed to be unreliable are replaced with those of an undisturbed second-order Stokes wave.

Results of detailed hydrodynamic analysis are also compared with those from a simpler numerical method, which uses a multi-column model of the semi-submersible platform to compute the diagonal of the quadratic transfer function matrix. To use the results from this simpler model, another new approach to extrapolating hydrodynamic analysis results is proposed: unknown off-diagonal terms of the quadratic transfer function matrix are estimated from the known on-diagonal terms. The results of each analysis are critically compared. The overall goal is to demonstrate the numerical impact of: 1) performing a very detailed second-order diffraction analysis, 2) performing a simplified second-order diffraction analysis, or 3) ignoring second-order diffraction entirely.

KEY WORDS:

airgap, second-order diffraction, semi-submersible, extremes

INTRODUCTION AND BACKGROUND

Airgap modeling is of concern for both fixed and floating structures, but it is particularly challenging in the case of floating structures because of their large volumes and the resulting effects of wave diffraction and radiation. Standard airgap response prediction uses linear theory, which generally does not effectively reproduce measurements from model tests. First-order diffraction is considerably less demanding than second-order, so use of only first-order diffraction merits some consideration. Second-order diffraction effects are expected to better reflect observed data. However, these radiation/diffraction panel calculations are very sensitive to the numerical modeling.

The cost of increasing the airgap for a semi-submersible is considerably higher than that for a fixed structure. Hence, instead of increasing the still-water airgap, it may be less expensive to strengthen the underside of the deck to withstand rare negative airgap events. In order to know the wave load and where impact will occur, reliable prediction tools are important. Model tests are often performed as part of the design of a new semi-submersible. If so, these calculations are needed to determine the locations at which airgap probes should be placed on the model.

Here, the numerical impact of modeling second-order diffraction effects is assessed by comparing various predictions of the statistical behavior of the free surface. Two hydrodynamic computer programs are employed: WAMIT 4.0 (1995), a second-order panel diffraction program, and WACYL (Birknes, 2000), a simpler second-order diffraction program. All analysis and model test results presented here are relevant to the Veslefrikk semisubmersible, the plan view of which is shown in Figure 1. Other relevant particulars for the vessel as analyzed include: draft: 23 m, displacement: 40,692 tonnes, airgap to still water level: 17.5 m and water depth on location: 175 m.

AIRGAP NOTATION AND VESLEFRIKK MODEL

The airgap, $a(t)$, can be considered a linear combination of three terms: a_0, the still-water airgap distance, $\eta(t)$, the wave surface elevation at a particular location along the structure measured with respect to a fixed observer, and $\delta(t)$ the corresponding vertical motion of the platform.

Among the various terms in the equation $a(t) = a_0 - [\eta(t) - \delta(t)]$, the vertical offset due to rigid body motion of the vessel, $\delta(t)$, is perhaps the most straightforward to model. Linear diffraction theory may often suffice to accurately model this offset. In contrast, the free surface elevation, $\eta(t)$, generally shows nonlinear behavior—and hence represents a non-Gaussian process. Modeling attention is therefore focused here on $\eta(t)$.

Specifically, $\eta(t)$ is assumed to be a sum of incident and diffracted

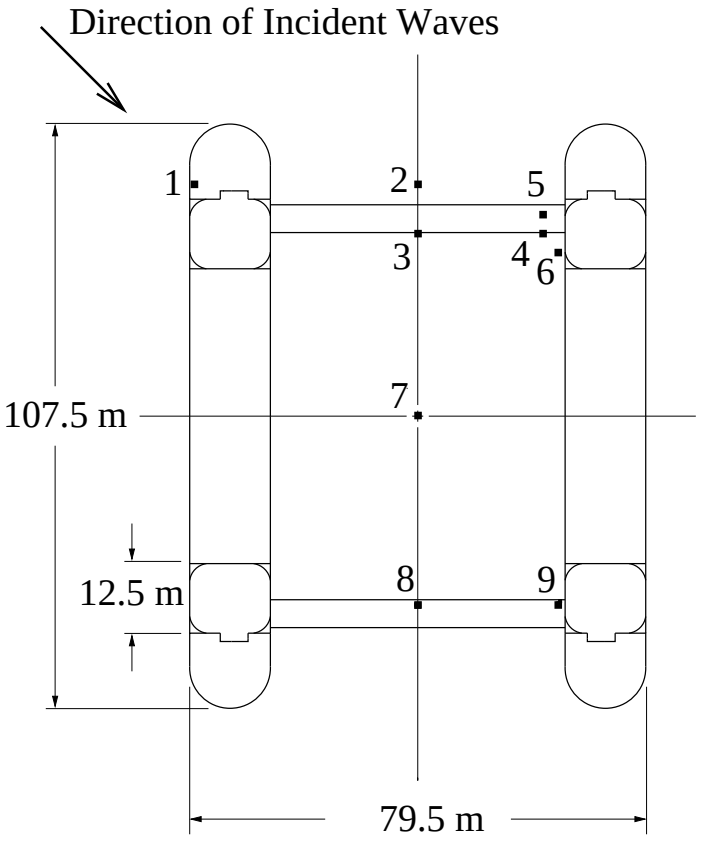

Figure 1: Plan view of Veslefrikk platform and location of airgap probes.

waves, η_i and η_d, each of which is a sum of first- and second-order components. This assumption is applied in both WAMIT and WACYL and is consistent with most state-of-the-art nonlinear hydrodynamic analyses, which generally employ second-order perturbation solutions.

Model test data used for verification of the hydrodynamic analysis come from a 1:45 length-scale model of Veslefrikk. Tests were performed in the wave tank at Marintek using various types of irregular waves (Fokk, 1995). Figure 1 shows a plan view of the platform, together with the 9 locations for which the airgap responses have been measured as a function of time. Note that airgap probes with lower numbers are generally further up-stream, i.e., closer to the wave generator. All tests studied here apply long-crested waves traveling along the diagonal of the structure.

The relative airgap at each of the wave-probe locations and the platform rigid-body motions have been recorded. The rigid body motions permit estimation of the net vertical displacement, $\delta(t)$, at any field-point location (x,y). This estimate is then subtracted from the measured airgap to determine the absolute wave elevation, $\eta(t)$, with respect to a fixed observer. This result is used for comparison with analytical predictions which assume a motionless structure.

WAMIT SECOND-ORDER DIFFRACTION ANALYSIS

The second-order panel diffraction program, WAMIT 4.0 (1995), was used to analyze Veslefrikk. The semi-submersible is symmetric about each of its transverse and longitudinal axis. Figure 2 shows both coarse and fine numerical models used in two separate WAMIT analyses. The coarse model includes 524 panels in each quadrant, while the fine includes 2066.

The full second-order quadratic transfer functions (QTF's) covering n discrete frequencies, f_n, is an $n \times n$ matrix of complex numbers, which can be represented as two separate $n \times n$ matrices: one of magnitudes and one of phases. The magnitude and phase transfer function matrices for wave probe locations 1 and 6 are shown in Figure 3. Each intersection of the mesh on the figure represents a single term in the QTF matrix.

A more simplified representation of these transfer functions which is useful for comparison purposes can be made by considering only the on-diagonal terms of the matrix, i.e. only those terms $H_2^+(f_1, f_2)$ for which $f_1 = f_2$. Figure 4 is such a representation, with abscissa $t_1 = t_2$, where $t_1 = 1/f_1$ and $t_2 = 1/f_2$. On Figure 4, the line marked "Stokes Theory" represents the QTF implied by Stokes' second-order wave theory only, and does not consider any diffraction effects associated with the presence of the structure. The results denoted "WAMIT - Fine" arise from the finer of the two meshes presented in Figure 2 and the "WAMIT - Coarse" results are from the more coarse of the two. The WAMIT analysis with the more fine physical mesh was analyzed over a finer set of frequencies as well (Δf = 0.0045 Hz vs 0.01 Hz). It is apparent from these figures that the more coarse physical mesh had some effect on the QTF results at each frequency analyzed, and that the finer frequency mesh captured frequency-dependent behavior which the coarser frequency mesh did not seek to evaluate.

The vertical scale of Figure 4 is truncated at $|H_2^+(t_1,t_2)| = 0.3$ to show the detailed behavior of the QTF diagonals. However, at very low periods the coarse mesh QTF magnitudes grow considerably larger for all filed-point locations. Figure 5 repeats the plot of $|H_2^+(t_1,t_2)|$ for locations 6 and 9, except that a log-scale is applied. At location 6, $|H_2^+(t_1,t_2)|$ reaches a maximum of 27, and at location 9, $|H_2^+(t_1,t_2)|$ reaches a maximum of 21. Inclusion of such large QTF values at low-periods yields dramatic overestimation of response amplitude relative to model test results. This overestimation may be due to over-prediction of true second-order effects, or due to omission of even higher order effects that may serve to reduce the response. Results for the finer mesh were not calculated using this model below a period of about 8 seconds. Subsequent diffraction calculations with a more refined model have yielded results similar to those of the coarse mesh; e.g. large values in the low period range.

STATISTICAL AIRGAP PREDICTION

The WAMIT results, as presented in Figures 3 and 4, are used in conjunction with a specified seastate to directly calculate the statistics of the airgap response. These statistical moments are calculated using the methods originated by Kac & Seigert (1947) and later expanded by Næss. The first- and second-order processes $\eta_1(t)$ and $\eta_2(t)$ are rewritten in terms of standard Gaussian processes.

$$\eta_1(t) = \sum_{j=1}^{2n} c_j u_j(t); \quad \eta_2(t) = \sum_{j=1}^{2n} \lambda_j u_j^2(t) \tag{1}$$

in which n is the number of frequency components of $\eta_1(t)$.

The coefficients c_j and λ_j can be obtained by solving an eigenvalue problem of size n for problems involving difference or sum frequencies only (Næss, 1986, Næss, 1992). Problems such as these, which involve both sum and difference frequencies, lead to eigenvalue problems of size $2n$, twice the number of frequency components of $\eta_1(t)$. Implementation of the theory is described in Winterstein *et al.*, 1994, with extensions to airgap analysis from Manuel & Winterstein, 2000.

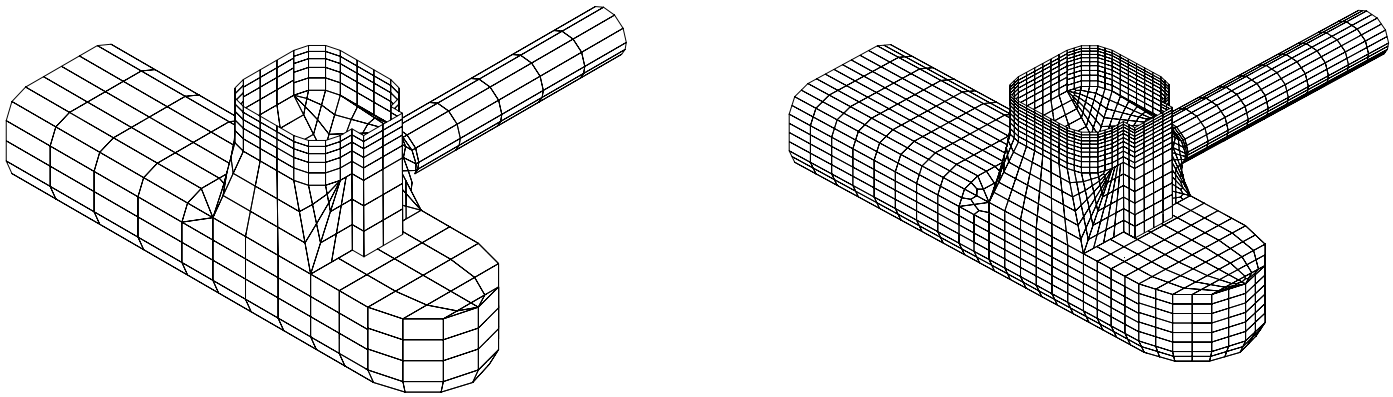

Coarse Hull Mesh Fine Hull Mesh

Figure 2: Comparison of Meshing Options used in WAMIT Analysis

The resulting moments of η can be found directly from the coefficients c_j and λ_j:

$$\sigma_\eta^2 = \sum_{j=1}^{2n} (c_j^2 + \lambda_j^2) \quad (2)$$

$$\alpha_{3,\eta} = \frac{1}{\sigma_x^3} \sum_{j=1}^{2n} (6c_j^2\lambda_j + 8\lambda_j^3) \quad (3)$$

$$\alpha_{4,\eta} = 3 + \frac{1}{\sigma_x^4} \sum_{j=1}^{2n} (48c_j^2\lambda_j^2 + 48\lambda_j^4) \quad (4)$$

This method of direct statistical calculation is used to produce the WAMIT statistical moment results shown in Figure 6. The plot of peaks is calculated as follows: The expected maximum of a standard Gaussian process in N cycles (e.g., Crandall & Mark, 1963) is first determined. The Hermite model (e.g.,Winterstein, 1988) is then applied using the theoretical skewness ($\alpha_{3,\eta}$)and kurtosis ($\alpha_{4,\eta}$) estimates from the Equations 3 and 4 to transform this Gaussian maximum to predict the non-Gaussian extreme value. Results presented here use an optimization routine to minimize error in matching skewness and kurtosis values. These analytical results predict mean 3-hour maxima, which are compared in Figure 6 with average maxima over 5 separate 3-hour model tests.

Recall from the discussion of Figure 4 that the WAMIT QTF's grow exceedingly large at low periods. As noted, use of these values leads to dramatic over-prediction of the response. It is hypothesized that superior prediction results can be obtained by using the WAMIT QTF's only over the range for which they appear reasonable: in this case, periods greater than about 8 seconds. Fortunately, the peak of the input wave spectrum is well within this period range for these model tests.

For periods less than a cut-off period, T_c, of about 8 seconds, the WAMIT QTF's are not used. Simply zeroing-off the unused QTF's would be straight-forward, but the actual QTF's below T_c are believed to be non-zero. Somehow extrapolating those QTF's believed to be reasonable may be another possibility, but the details of a valid QTF extrapolation may be somewhat arbitrary. QTF's as predicted from Stokes theory have several properties that make them a reasonable substitution for unusable QTF's predicted by diffraction.

Stokes theory is well known and the QTF's can be calculated analytically. Stokes QTF's have previously been applied in conjunction with linear diffraction results over the entire frequency range (Sweetman & Winterstein, 2001). It was found that this combination results in better predictions of the maximum water surface elevation than does use of the linear diffraction results alone. It is recognized that Stokes transfer functions ignore diffraction effects, which are potentially most important for small period waves. However, they are used here since reliable prediction of diffraction effects is not available.

In the present analysis, Stokes QTF's were substituted for the WAMIT QTF if the average of the frequency pair, $\frac{1}{2}(f_1 + f_2)$, is greater than a cut-off frequency, $f_c = 1/T_c$. The selection of this form for the cut-off will be discussed later. Cut-off periods of T_c = 7, 8 and 9 seconds each have been applied, and the results are compared in Figure 6. "Coarse Mesh above 7 sec," noticeably over-predicts at all locations. This observed over-prediction, relative to T_c = 8 or 9 seconds and to measured data, confirms that the WAMIT results should not be trusted for periods as low as 7 seconds.

As can also be observed in the figure, second-order diffraction has only a minor effect on the standard deviation, i.e. the rms response of the process. It appears that linear diffraction alone (calculated here using the fine mesh) may be sufficient to accurately predict the rms level of the wave elevation, and hence that of the airgap response. However, the values of the coefficients of skewness and kurtosis both deviate substantially from their respective Gaussian values of 0 and 3.

The non-Gaussian effects associated with increased values of the coefficients of skewness and kurtosis substantially increases the prediction of the mean maximum from the "First-Order Only" result to approximately that of the observed model test data ("Measured"). The magnitude of the predicted peak is generally centered amongst the measured data. However, even these second-order predictions fail to adequately follow the trend in observed extremes at near-column locations. The discrepancy is particularly severe at locations 1, 5 and 9. At these locations, a run-up effect is expected to be important, and this is an effect which is not handled by the present analysis. Locations 4 and 6 will also have some influence of run-up.

Ignoring the T_c = 7 second results, comparable results are obtained from the second-order analysis using T_c equal to either 8 or 9 seconds, with either the coarse or fine mesh. Each of these analyses yield about

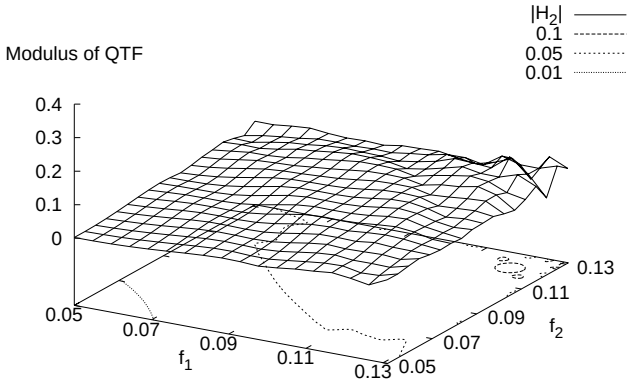

Modulus - Location 1

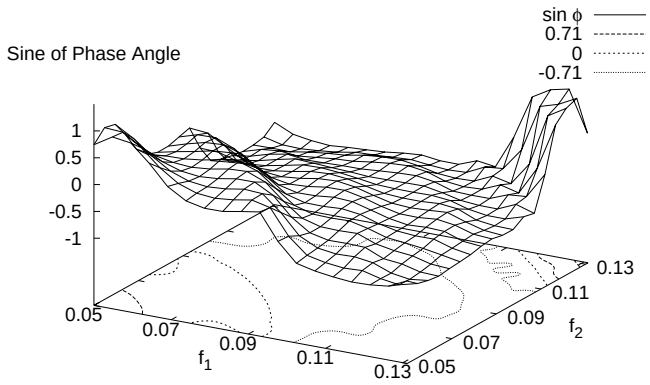

Phase - Location 1

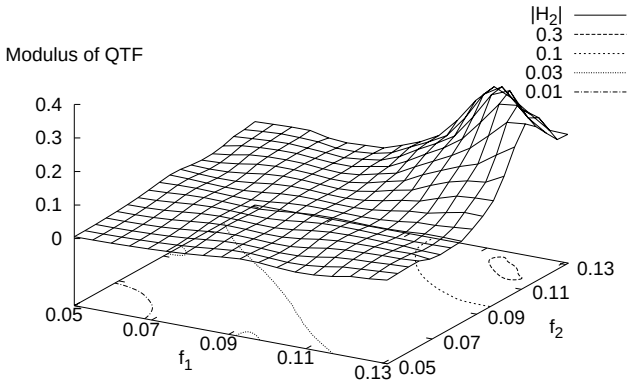

Modulus - Location 6

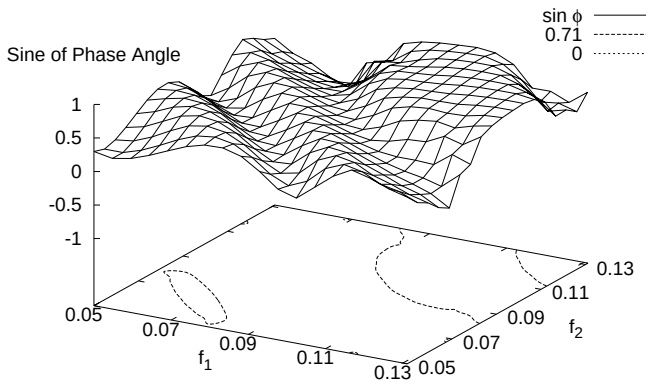

Phase - Location 6

Figure 3: Modulus and Phase of Second-Order Quadratic Transfer Functions from WAMIT

the same level of agreement with the measured data. In particular, considering the mean maximum predicted airgap response, there is almost no difference between results for the coarse and fine meshing options for frequencies above 9 seconds, and only relatively slight differences between these results and those for the fine mesh above 8 seconds. Thus, these results are not found to be particularly sensitive to the mesh density. As long as the very low period QTF's were not used ($T_c < 8$ seconds), all prediction results, regardless of modeling assumptions, show better agreement with measured data than results based on first-order alone. Thus, use of second-order diffraction should be considered in practical design work if the airgap response is believed to be a critical design quantity.

WACYL MULTI-COLUMN ANALYSIS

Second-order diffraction theory can be applied to a far simpler model than that used in the WAMIT analysis presented earlier. In the simplified analysis, the model of the Veslefrikk platform consists of 4 vertical circular cylinders of diameter 12.5 m. Transfer functions for the diffracted wave surface are calculated only *at* the column surface. The analysis does not consider the non-circular shape of the actual columns nor does it consider the presence of pontoons.

The program WACYL, of Det Norske Veritas, written by Birkes (2000), was used to perform this hydrodynamic analysis. Malencia *et al.*, (1999) outline this second-order theory which describes waves against an array of vertical, bottom-mounted and fixed cylinders. Perturbation techniques and potential theory are used and only sum-frequency terms are considered. It is assumed that the wave field is monochromatic and that the depth is finite. The present WACYL implementation of the multi-column method calculates only on-diagonal QTF terms.

Two sensitivity studies were performed as part of this analysis. In each study, the free surface containing all of the cylinders was discretized with quadrilateral panels. It was determined that accurate results for this configuration could be obtained using a mesh of 28 616 panels, and an analysis using 20 Fourier modes.

The results of the WACYL analysis are presented in Figure 7. Like Figure 4, Figure 7 shows comparisons between diagonals of QTF matrices. Here, results from WAMIT calculations are compared with results from WACYL. The WACYL results show reasonable agreement with the WAMIT results except at location 9, where WACYL under-predicts

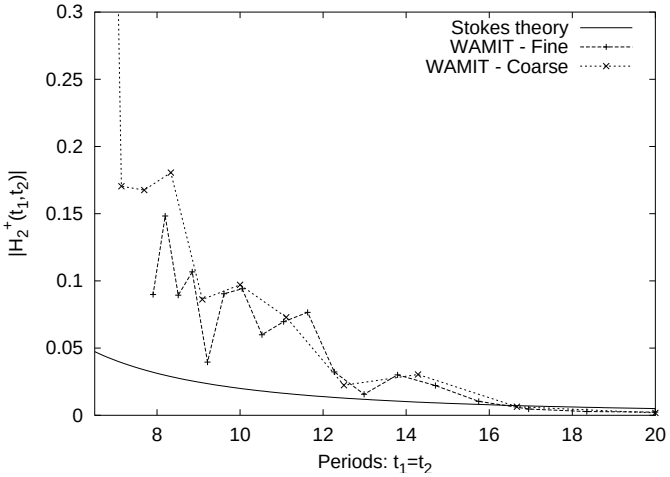

Location 1

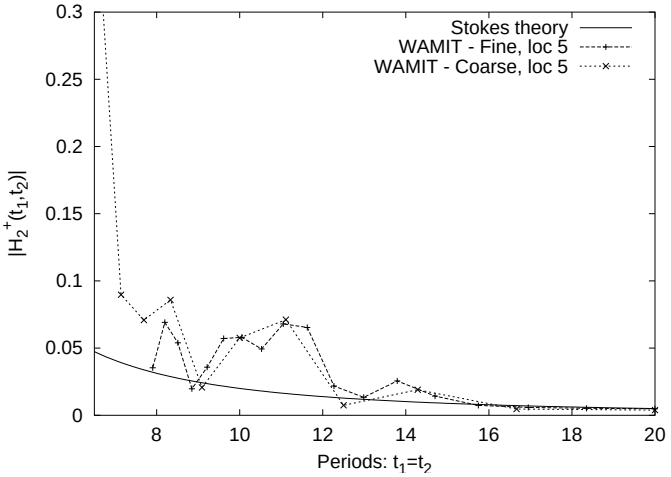

Location 5

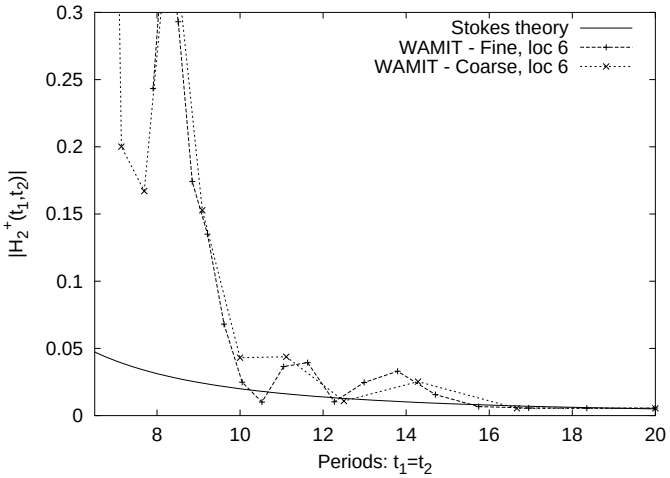

Location 6

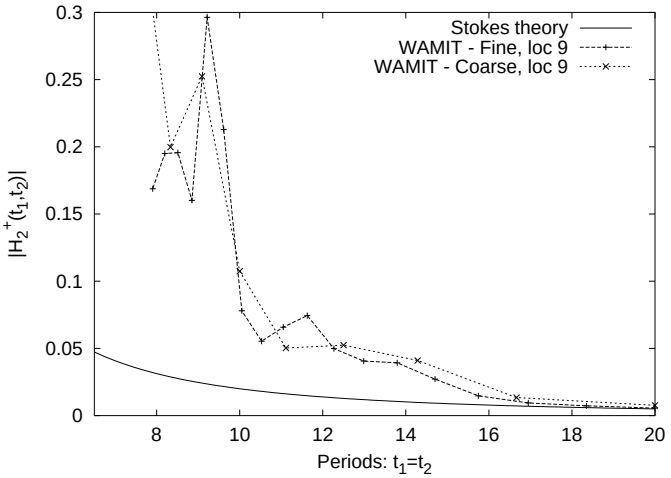

Location 9

Figure 4: Diagonals of WAMIT Quadratic Transfer Function Matrix

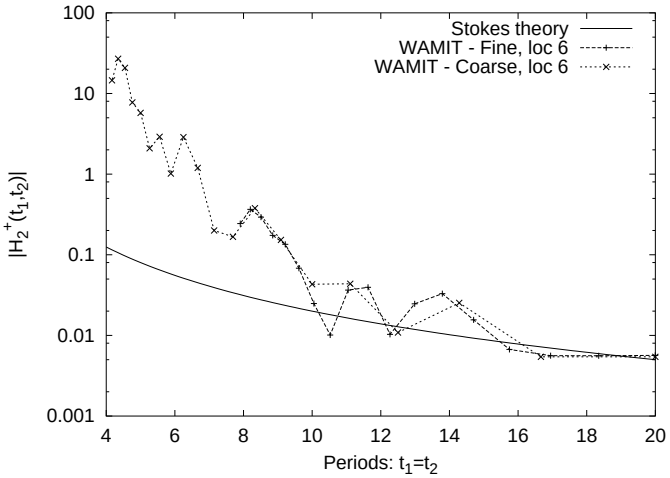

Location 6

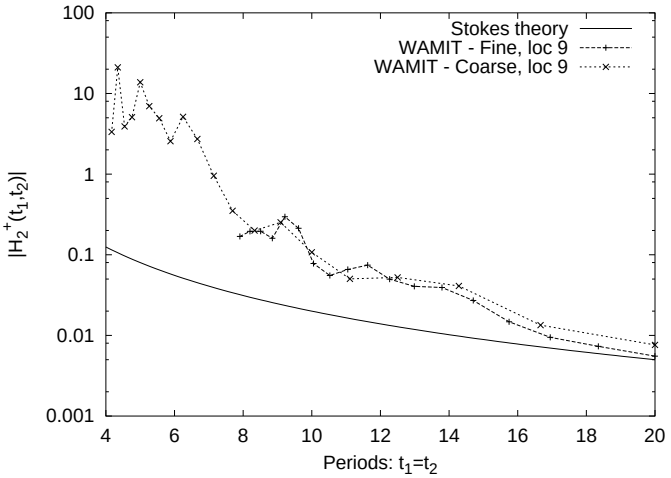

Location 9

Figure 5: Log-Scale: Diagonals of WAMIT Quadratic Transfer Function Matrix

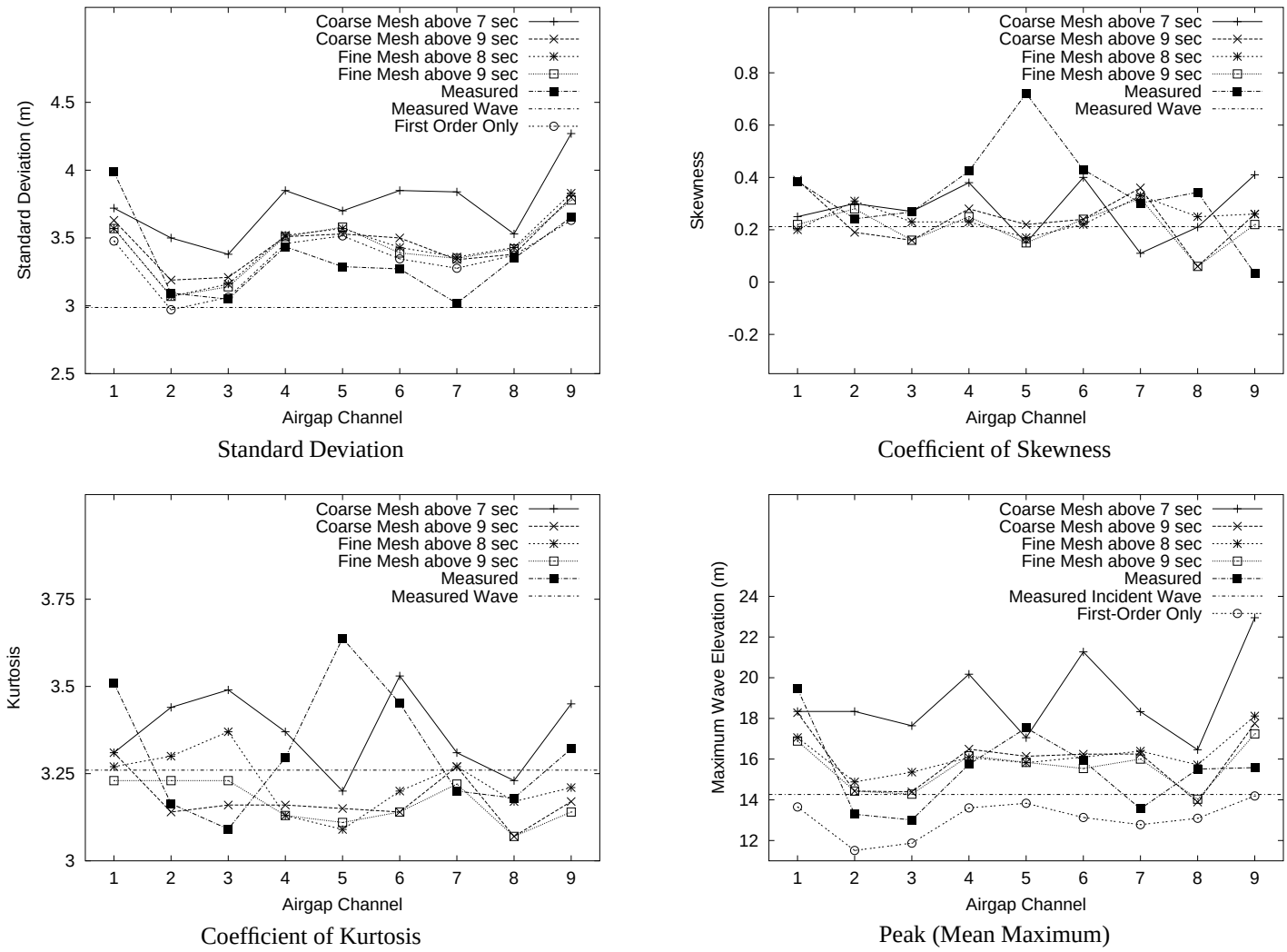

Figure 6: Results based on using WAMIT second-order transfer function results with Stokes second order transfer functions for low periods. H_s = 12 meters, T_p = 11.5 seconds

WAMIT by a considerable margin. Considering *only* the modulus of the QTF diagonals may be misleading in this case, however, because the integrated effect of the QTF's only slightly under-predicts the mean maximum, as shown later in Figure 8. This result may be due to the off-diagonal terms calculated by WAMIT or due to the effects of relative phases.

Off-diagonal QTF's are not produced by WACYL but are needed to produce results comparable to those presented in Figure 6. A new method is proposed to approximate these off-diagonals from on-diagonal terms. Referring back to Figure 3, it appears that both the modulus and phase of the QTF remain reasonably constant along lines of constant $f_1 + f_2$. This behavior has been verified to be typical of all near-column locations for this set of WAMIT QTF's. Each on-diagonal term produced by WACYL is hence used here to estimate off-diagonal terms as $H_2^+(f_1, f_2) = H_2^+(f_d, f_d)$, if $f_1 + f_2 = 2f_d$, where f_d is that frequency associated with each diagonal term of the QTF matrix. The same observation of near-constant $H_2^+(f_1, f_2)$ for constant $(f_1 + f_2)$ was also used to select the form of the high-frequency cut-off used previously.

After estimating all off-diagonal terms of the QTF matrix, transfer functions from the multi-column method are applied to a wave spectrum as in previous calculations for Figure 6. The subsequent statistical moments are compared with analogous results from WAMIT and from model tests in Figure 8. Because calculations are available only at the column surface, results are shown only for locations 1, 4, 5, 6 and 9. One set of multi-column results include phase effects and another assumes all second-order components are phase-locked. It is readily apparent that results are sensitive to relative phase effects. One concern is noted: the multi-column method including relative phases predicts an extremely low skewness (-0.27), and a high kurtosis (3.75) at location 6, which is not yet adequately understood.

CONCLUSIONS

A semisubmersible production platform, the Veslefrikk, has been analyzed using two different hydrodynamic computer programs, WAMIT and WACYL. Each code used a different implementation of second-order hydrodynamic theory to predict diffraction quadratic transfer functions of the free surface.

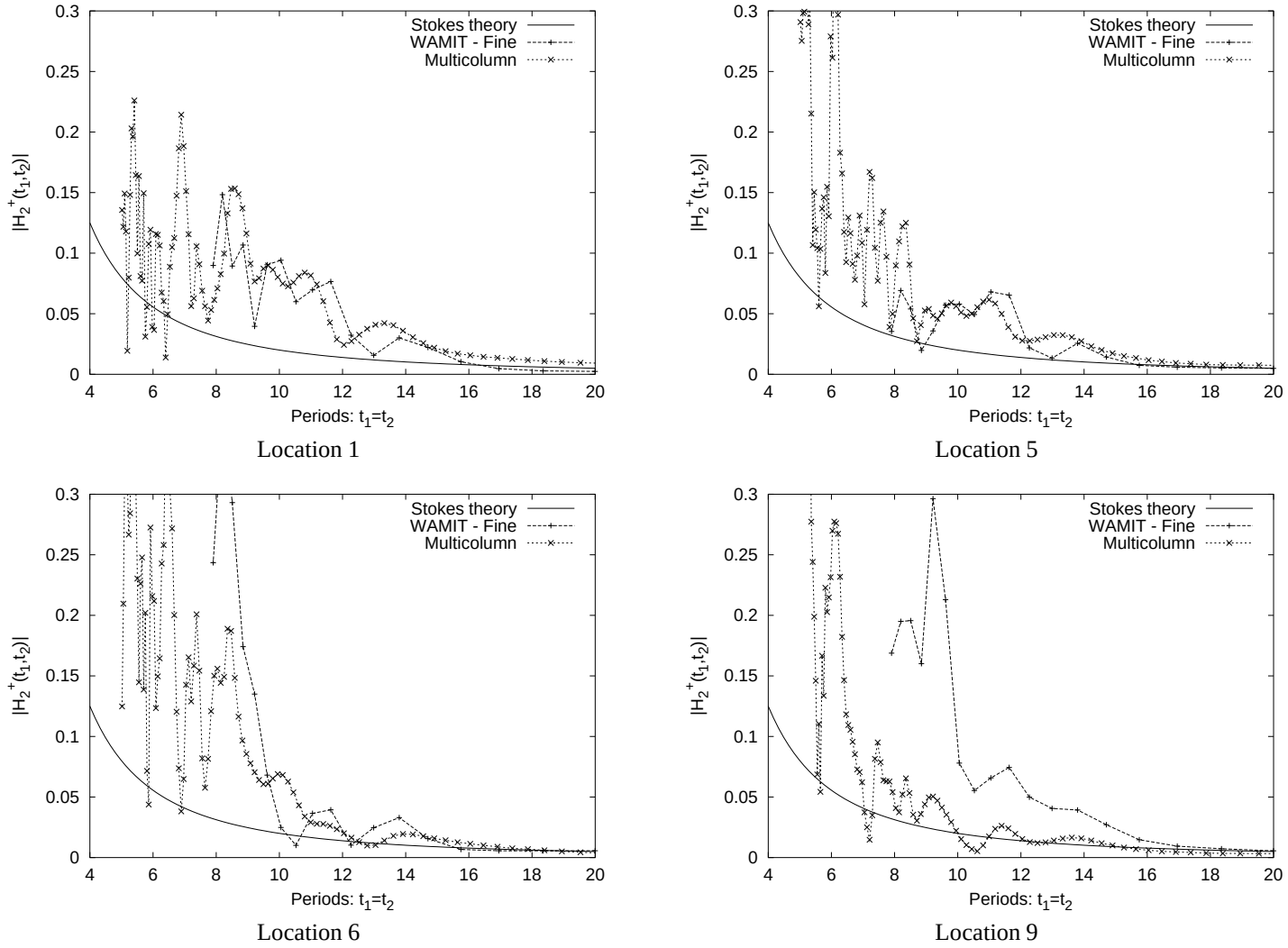

Figure 7: Second-Order Transfer Function Results based on Multi-Column Method

The first hydrodynamic analysis was performed using WAMIT. Second-order diffraction was found to yield considerably better peak predictions than first-order alone. Predictions of mean maxima were typically 20% higher than those based on first order only. As part of post-processing the WAMIT results, a new method has been introduced by which unknown high-frequency QTF's are approximated by those predicted by Stokes wave theory. Two different mesh densities were applied to both the body and the free surface, and the hydrodynamic results were not found to be very sensitive to the mesh density or the maximum frequency below which second-order WAMIT results are considered.

As long as very high frequency QTF's are not used, all prediction results based on Second-order diffraction, regardless of modeling assumptions, show better agreement with measured data than results based on first-order alone. Thus, use of second-order diffraction should be considered in practical design work if the airgap response is believed to be a critical design quantity.

The second hydrodynamic analysis was performed using the program WACYL, and a simplified model of the semisubmersible consisting of an array of fixed bottom-mounted vertical circular cylinders. This analysis was found to be more accurate on average than a first-order analysis using a more detailed model, though results are somewhat unpredictable. As part of the post-processing of these results, a new method has been introduced in which unknown off-diagonal quadratic transfer function terms are approximated from known on-diagonal terms. The effects of relative phase of the second-order components were found to have a major impact on the results of the simplified hydrodynamic analysis.

WACYL appears able to predict results that are generally qualitatively similar to WAMIT, despite its neglect of structural details, at a far less computational cost. In many cases WACYL is seen to predict larger nonlinear effects (e.g., skewness, kurtosis, maxima). Multi-column analysis appears to deserve additional study.

Whether estimated by WAMIT, WACYL, or other means, higher-order effects can significantly increase predicted levels of airgap demand, and this increase in predicted demand improves prediction agreement with model test results.

ACKNOWLEDGEMENTS

The authors gratefully acknowledge the support of the Reliability of Marine Structures (RMS) program at Stanford University, and of Norske Hydro, who supported the implementation of WACYL at DNV.

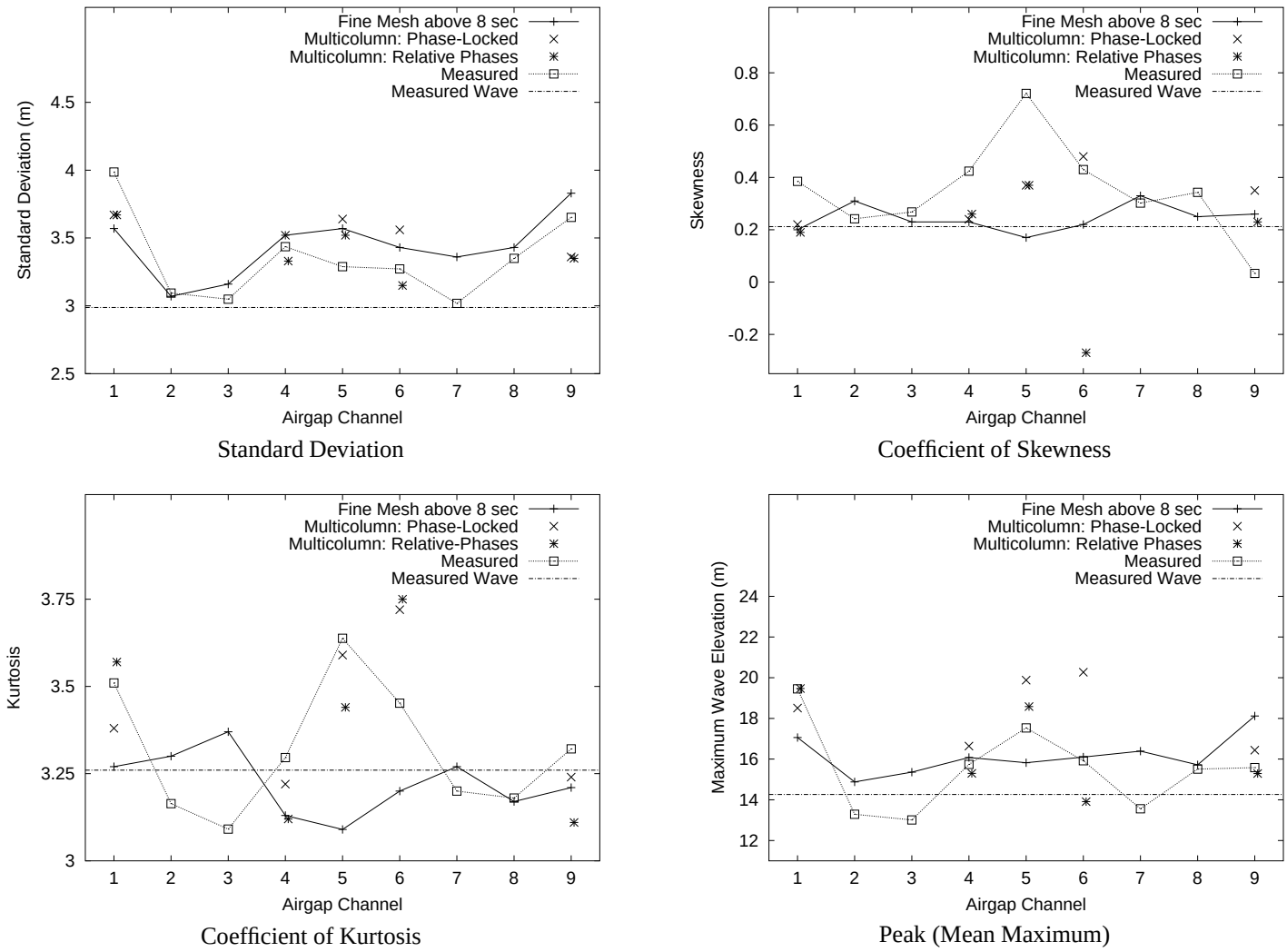

Figure 8: Results based on using WAMIT second-order transfer function results with Stokes second order transfer functions for low periods compared with Multi-column Results H_s = 12 meters, T_p = 11.5 seconds

REFERENCES

Birknes, Jørn. 2000. *A Convergence Study of Second-Order Wave Elevation on Four Cylinders. Second-Order Forces and Moments.* Report no. 2000-3455. Det Norske Veritas.

Crandall, S. H., & Mark, W. D. 1963. *Random Vibration in Mechanical Systems*. Monograph. Academic Press.

Fokk, T. 1995. *Veslefrikk B Air Gap Model Tests*. Tech. rept. 512167.00.01. MARINTEK Trondheim, Norway.

Kac, M., & Seigert, A. J. F. 1947. On the theory of noise in radio receivers with square law detectors. *Journal of Applied Physics*, 383–400.

Malenica, Š, Eatock Taylor, R, & Huang, J B. 1999. Second-order water wave diffraction by an array of vertical cylinders. *J. Fluid Mechanics, vol. 390, pp. 349-373.*

Manuel, Lance, & Winterstein, Steven R. 2000. Reliability Based Predictions of a Design Air Gap for Floating Offshore Structures. *In: Proceedings 8'th ASCE Conf. on Probablistic Mechanics and Structural Reliability*. ASCE.

Næss, A. 1986. The Statistical Distribution of Second-Order Slowly-Varying Forces and Motions. *Applied Ocean Research*, **8**, 110–118.

Næss, A. 1992. Prediction of extremes related to the second-order, sum-frequency response of a TLP. *Pages 436–443 of: Proc., 2nd Intl. Offshore Polar Eng*. ISOPE.

Sweetman, B., & Winterstein, S. R. 2001. Non-Gaussian Air Gap Response Models for Floating Structures. *Journal of Engineering Mechanics*. Submitted for Review.

WAMIT 4.0. 1995. *WAMIT: A Radiation-Diffraction Panel Program for Wave-Body Interactions–User's Manual*. Dept. of Ocean Engineering, M.I.T.

Winterstein, S. R. 1988. Nonlinear vibration models for extremes and fatigue. *Journal of Engineering Mechanics, ASCE*, **114**(10).

Winterstein, S.R., T.C., Ude, & Marthinsen, T. 1994. Volterra Models of Ocean Structures: Extreme and Fatigue Reliability. *Journal of Engineering Mechanics*, **120**(6), 1369–1385.